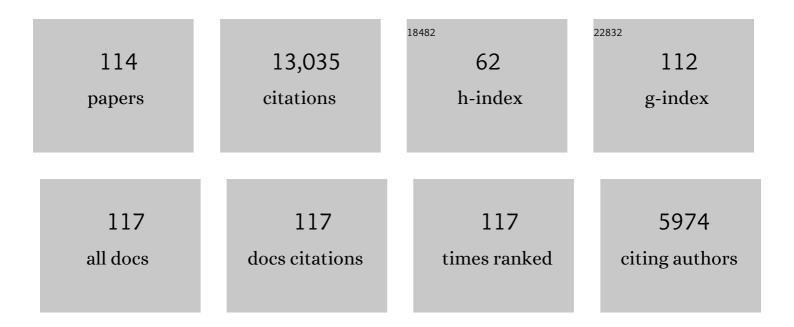
Barry E Parsons

List of Publications by Year in descending order

Source: https://exaly.com/author-pdf/57627/publications.pdf Version: 2024-02-01



#	Article	IF	CITATIONS
1	An analysis of the variation of ocean floor bathymetry and heat flow with age. Journal of Geophysical Research, 1977, 82, 803-827.	3.3	2,489
2	Toward mapping surface deformation in three dimensions using InSAR. Geophysical Research Letters, 2004, 31, .	4.0	560
3	Mantle convection and the thermal structure of the plates. Journal of Geophysical Research, 1978, 83, 4485-4496.	3.3	501
4	Oceans and continents: Similarities and differences in the mechanisms of heat loss. Journal of Geophysical Research, 1981, 86, 11535-11552.	3.3	349
5	On the interaction of two scales of convection in the mantle. Journal of Geophysical Research, 1975, 80, 2529-2541.	3.3	338
6	InSAR Observations of Low Slip Rates on the Major Faults of Western Tibet. Science, 2004, 305, 236-239.	12.6	305
7	Multi-interferogram method for measuring interseismic deformation: Denali Fault, Alaska. Geophysical Journal International, 2007, 170, 1165-1179.	2.4	293
8	Surface displacements and source parameters of the 2003 Bam (Iran) earthquake from Envisat advanced synthetic aperture radar imagery. Journal of Geophysical Research, 2005, 110, .	3.3	240
9	The relationship between surface topography, gravity anomalies, and temperature structure of convection. Journal of Geophysical Research, 1983, 88, 1129-1144.	3.3	210
10	InSAR slip rate determination on the Altyn Tagh Fault, northern Tibet, in the presence of topographically correlated atmospheric delays. Geophysical Research Letters, 2008, 35, .	4.0	202
11	Crustal strain in central Greece from repeated GPS measurements in the interval 1989-1997. Geophysical Journal International, 1998, 135, 195-214.	2.4	188
12	The motion of crustal blocks driven by flow of the lower lithosphere and implications for slip rates of continental strike-slip faults. Nature, 1998, 391, 655-659.	27.8	185
13	Comparison of long-wavelength residual elevation and free air gravity anomalies in the North Atlantic and possible implications for the thickness of the lithospheric plate. Journal of Geophysical Research, 1975, 80, 1031-1052.	3.3	181
14	Measurement of interseismic strain accumulation across the North Anatolian Fault by satellite radar interferometry. Geophysical Research Letters, 2001, 28, 2117-2120.	4.0	178
15	The 2009 L'Aquila earthquake (central Italy): A source mechanism and implications for seismic hazard. Geophysical Research Letters, 2009, 36, .	4.0	174
16	Causes and consequences of the relation between area and age of the ocean floor. Journal of Geophysical Research, 1982, 87, 289-302.	3.3	173
17	Geodetic determination of tectonic deformation in central Greece from 1900 to 1988. Nature, 1991, 350, 124-129.	27.8	172
18	The 2003 Bam (Iran) earthquake: Rupture of a blind strike-slip fault. Geophysical Research Letters, 2004, 31, n/a-n/a.	4.0	152

#	Article	IF	CITATIONS
19	Crustal deformation during 1994-1998 due to oblique continental collision in the central Southern Alps, New Zealand, and implications for seismic potential of the Alpine fault. Journal of Geophysical Research, 1999, 104, 25233-25255.	3.3	151
20	Deformation of western Turkey from a combination of permanent and campaign GPS data: Limits to blockâ€like behavior. Journal of Geophysical Research, 2009, 114, .	3.3	148
21	Extension on the Tibetan plateau: recent normal faulting measured by InSAR and body wave seismology. Geophysical Journal International, 2010, 183, 503-535.	2.4	146
22	Planform of mantle convection beneath the Pacific Ocean. Nature, 1980, 288, 442-446.	27.8	145
23	Source parameters of the 1 October 1995 Dinar (Turkey) earthquake from SAR interferometry and seismic bodywave modelling. Earth and Planetary Science Letters, 1999, 172, 23-37.	4.4	144
24	The 1998 March 14 Fandoqa earthquake (Mw6.6) in Kerman province, southeast Iran: re-rupture of the 1981 Sirch earthquake fault, triggering of slip on adjacent thrusts and the active tectonics of the Gowk fault zone. Geophysical Journal International, 2001, 146, 371-398.	2.4	144
25	A new velocity field for Greece: Implications for the kinematics and dynamics of the Aegean. Journal of Geophysical Research, 2010, 115, .	3.3	144
26	The 1994 Sefidabeh (eastern Iran) earthquakes revisited: new evidence from satellite radar interferometry and carbonate dating about the growth of an active fold above a blind thrust fault. Geophysical Journal International, 2006, 164, 202-217.	2.4	143
27	A relation between the driving force and geoid anomaly associated with mid-ocean ridges. Earth and Planetary Science Letters, 1980, 51, 445-450.	4.4	141
28	Post-seismic motion following the 1997 Manyi (Tibet) earthquake: InSAR observations and modelling. Geophysical Journal International, 2007, 169, 1009-1027.	2.4	141
29	Displacement field and slip distribution of the 2005 Kashmir earthquake from SAR imagery. Geophysical Research Letters, 2006, 33, .	4.0	138
30	Geodetic strain of Greece in the interval 1892-1992. Journal of Geophysical Research, 1997, 102, 24571-24588.	3.3	128
31	Evolution of Santorini Volcano dominated by episodic and rapid fluxes of melt from depth. Nature Geoscience, 2012, 5, 749-754.	12.9	127
32	Venus Tectonics: Initial Analysis from Magellan. Science, 1991, 252, 297-312.	12.6	118
33	Triggered slip: Observations of the 17 August 1999 Izmit (Turkey) Earthquake using radar interferometry. Geophysical Research Letters, 2001, 28, 1079-1082.	4.0	110
34	Highâ€Resolution Surface Velocities and Strain for Anatolia From Sentinelâ€I InSAR and GNSS Data. Geophysical Research Letters, 2020, 47, e2020GL087376.	4.0	108
35	Slip in the 2010–2011 Canterbury earthquakes, New Zealand. Journal of Geophysical Research, 2012, 117, .	3.3	103
36	The rates of plate creation and consumption. Geophysical Journal International, 1981, 67, 437-448.	2.4	100

#	Article	IF	CITATIONS
37	Heat flow observations on the Bermuda Rise and thermal models of midplate swells. Journal of Geophysical Research, 1986, 91, 3701-3723.	3.3	96
38	The Reykjanes Ridge: structure and tectonics of a hot-spot-influenced, slow-spreading ridge, from multibeam bathymetry, gravity and magnetic investigations. Earth and Planetary Science Letters, 1998, 160, 463-478.	4.4	96
39	Geodetic estimate of seismic hazard in the Gulf of Korinthos. Geophysical Research Letters, 1997, 24, 1303-1306.	4.0	94
40	Seismotectonic, rupture process, and earthquake-hazard aspects of the 2003 December 26 Bam, Iran, earthquake. Geophysical Journal International, 2006, 166, 1270-1292.	2.4	94
41	Mesozoic magnetic lineations in the Mozambique Basin. Earth and Planetary Science Letters, 1979, 43, 260-264.	4.4	88
42	Eocene to recent development of the South-west Indian Ridge, a consequence of the evolution of the Indian Ocean Triple Junction. Geophysical Journal of the Royal Astronomical Society, 1981, 64, 587-604.	0.2	87
43	Fault identification for buried strike-slip earthquakes using InSAR: The 1994 and 2004 Al Hoceima, Morocco earthquakes. Geophysical Journal International, 2006, 166, 1347-1362.	2.4	86
44	The Origin of Outer Topographic Rises Associated with Trenches. Geophysical Journal International, 1976, 45, 707-712.	2.4	85
45	The 2010 <i>M</i> _{<i>W</i>} 6.8 Yushu (Qinghai, China) earthquake: Constraints provided by InSAR and body wave seismology. Journal of Geophysical Research, 2011, 116, .	3.3	84
46	Features on Venus generated by plate boundary processes. Journal of Geophysical Research, 1992, 97, 13533-13544.	3.3	82
47	The Indian Ocean Triple Junction. Journal of Geophysical Research, 1980, 85, 4723-4739.	3.3	81
48	Crustal deformation of the Marlborough Fault Zone in the South Island of New Zealand: Geodetic constraints over the interval 1982-1994. Journal of Geophysical Research, 1998, 103, 30147-30165.	3.3	81
49	Geodetic investigation of the 13 May 1995 Kozani-Grevena (Greece) Earthquake. Geophysical Research Letters, 1997, 24, 707-710.	4.0	80
50	The 2011 Mw 7.1 Van (Eastern Turkey) earthquake. Journal of Geophysical Research: Solid Earth, 2013, 118, 1619-1637.	3.4	80
51	The Dahuiyeh (Zarand) earthquake of 2005 February 22 in central Iran: reactivation of an intramountain reverse fault. Geophysical Journal International, 2006, 164, 137-148.	2.4	79
52	Fault slip in the 1997 Manyi, Tibet earthquake from linear elastic modelling of InSAR displacements. Geophysical Journal International, 2007, 169, 988-1008.	2.4	78
53	Gravity anomalies derived from Seasat, Geosat, ERS-1 and TOPEX/POSEIDON altimetry and ship gravity: a case study over the Reykjanes Ridge. Geophysical Journal International, 1995, 122, 551-568.	2.4	77
54	Assessing the ability of Pleiades stereo imagery to determine height changes in earthquakes: A case study for the El Mayor ucapah epicentral area. Journal of Geophysical Research: Solid Earth, 2015, 120, 8793-8808.	3.4	77

#	Article	IF	CITATIONS
55	The effect of a shallow low viscosity zone on the apparent compensation of mid-plate swells. Earth and Planetary Science Letters, 1987, 82, 335-348.	4.4	76
56	The crustal structure of the Madagascar Ridge. Geophysical Journal International, 1981, 66, 351-377.	2.4	70
57	The vertical separation of mainshock rupture and microseismicity at Qeshm island in the Zagros fold-and-thrust belt, Iran. Earth and Planetary Science Letters, 2010, 296, 181-194.	4.4	67
58	Constraining crustal velocity fields with InSAR for Eastern Turkey: Limits to the blockâ€like behavior of Eastern Anatolia. Journal of Geophysical Research: Solid Earth, 2014, 119, 5215-5234.	3.4	67
59	From quiescence to unrest: 20 years of satellite geodetic measurements at Santorini volcano, Greece. Journal of Geophysical Research: Solid Earth, 2015, 120, 1309-1328.	3.4	67
60	The relationship between gravity and bathymetry in the Pacific Ocean. Geophysical Journal International, 1985, 83, 263-298.	2.4	66
61	Convective instabilities in a variable viscosity fluid cooled from above. Physics of the Earth and Planetary Interiors, 1985, 39, 14-32.	1.9	66
62	Dynamic topography and gravity anomalies for fluid layers whose viscosity varies exponentially with depth. Geophysical Journal International, 1987, 90, 349-368.	2.4	66
63	Limitations of rupture forecasting exposed by instantaneously triggered earthquake doublet. Nature Geoscience, 2016, 9, 330-336.	12.9	66
64	Global derivation of marine gravity anomalies from Seasat, Geosat, ERS-1 and TOPEX/POSEIDON altimeter data. Geophysical Journal International, 1998, 134, 449-459.	2.4	65
65	The 2005 Qeshm Island earthquake (Iran)-a link between buried reverse faulting and surface folding in the Zagros Simply Folded Belt?. Geophysical Journal International, 2007, 171, 326-338.	2.4	65
66	Observations of convection at rayleigh numbers up to 760,000 in a fluid with large prandtl number. Geophysical and Astrophysical Fluid Dynamics, 1977, 9, 201-217.	1.2	64
67	Aseismic deformation of a fold-and-thrust belt imaged by synthetic aperture radar interferometry near Shahdad, southeast Iran. Geology, 2004, 32, 577.	4.4	64
68	Effect of a shallow lowâ€viscosity zone on the formation of midplate swells. Journal of Geophysical Research, 1988, 93, 3144-3156.	3.3	59
69	Geodetic constraints on glacial isostatic adjustment in Europe. Geophysical Research Letters, 2005, 32,	4.0	58
70	Depth segmentation of the seismogenic continental crust: The 2008 and 2009 Qaidam earthquakes. Geophysical Research Letters, 2011, 38, n/a-n/a.	4.0	58
71	A major, intraplate, normalâ€faulting earthquake: The 1739 Yinchuan event in northern China. Journal of Geophysical Research: Solid Earth, 2016, 121, 293-320.	3.4	58
72	Rapid strain accumulation on the Ashkabad fault (Turkmenistan) from atmosphere orrected InSAR. Journal of Geophysical Research: Solid Earth, 2013, 118, 3674-3690.	3.4	57

#	Article	IF	CITATIONS
73	Interseismic strain accumulation across the North Anatolian Fault from Envisat InSAR measurements. Geophysical Research Letters, 2011, 38, n/a-n/a.	4.0	52
74	A note on the correction of ocean floor depths for sediment loading. Journal of Geophysical Research, 1982, 87, 4715-4722.	3.3	51
75	Seamount abundances and distributions in the southeast Pacific. Earth and Planetary Science Letters, 1988, 87, 137-151.	4.4	44
76	The postseismic response to the 2002 <i>M</i> 7.9 Denali Fault earthquake: constraints from InSAR 2003-2005. Geophysical Journal International, 2009, 176, 353-367.	2.4	42
77	An optimal procedure for deriving marine gravity from multi-satellite altimetry. Geophysical Journal International, 1996, 125, 705-718.	2.4	40
78	A method for the joint inversion of geodetic and seismic waveform data using ABIC: application to the 1997 Manyi, Tibet, earthquake. Geophysical Journal International, 2014, 196, 1564-1579.	2.4	40
79	Combining InSAR and seismology to study the 2003 Siberian Altai earthquakes-dextral strike-slip and anticlockwise rotations in the northern India-Eurasia collision zone. Geophysical Journal International, 2007, 169, 216-232.	2.4	38
80	The 2013 Balochistan earthquake: An extraordinary or completely ordinary event?. Geophysical Research Letters, 2015, 42, 6236-6243.	4.0	38
81	Bathymetry of the Reykjanes Ridge. Marine Geophysical Researches, 1997, 19, 55-64.	1.2	36
82	Relation between surface velocity field and shear wave splitting in the South Island of New Zealand. Journal of Geophysical Research, 2002, 107, ETG 5-1-ETG 5-7.	3.3	36
83	The 1998 Aiquile, Bolivia earthquake: A seismically active fault revealed with InSAR. Earth and Planetary Science Letters, 2005, 232, 39-49.	4.4	35
84	Seasatâ€derived gravity over the Musicians Seamounts. Journal of Geophysical Research, 1986, 91, 8325-8340.	3.3	33
85	Surface displacements in the September 2005 Afar rifting event from satellite image matching: Asymmetric uplift and faulting. Geophysical Research Letters, 2009, 36, .	4.0	33
86	Coseismic and postseismic displacements from the 1978 M w 7.3 Tabas-e-Golshan earthquake in eastern Iran. Earth and Planetary Science Letters, 2016, 452, 185-196.	4.4	33
87	Blind Thrusting, Surface Folding, and the Development of Geological Structure in the <i>M</i> _{<i>w</i>} 6.3 2015 Pishan (China) Earthquake. Journal of Geophysical Research: Solid Earth, 2017, 122, 9359-9382.	3.4	33
88	Placing bounds on lithospheric deformation in the central Pacific Ocean. Earth and Planetary Science Letters, 1992, 111, 123-139.	4.4	32
89	Interpreting gravity, geoid, and topography for convection with temperature dependent viscosity: Application to surface features on Venus. Journal of Geophysical Research, 1995, 100, 21155.	3.3	32
90	Seismotectonics and rupture process of the <i>M</i> _W Â7.1 2011 Van reverse-faulting earthquake, eastern Turkey, and implications for hazard in regions of distributed shortening. Geophysical Journal International, 2016, 206, 501-524.	2.4	30

#	Article	IF	CITATIONS
91	Time-dependent postseismic slip following the 1978 M 7.3 Tabas-e-Golshan, Iran earthquake revealed by over 20 years of ESA InSAR observations. Earth and Planetary Science Letters, 2018, 483, 64-75.	4.4	30
92	The 2006 March 25 Fin earthquakes (Iran)-insights into the vertical extents of faulting in the Zagros Simply Folded Belt. Geophysical Journal International, 2010, , .	2.4	29
93	Effect of a shallow lowâ€viscosity zone on smallâ€scale instabilities under the cooling oceanic plates. Journal of Geophysical Research, 1988, 93, 3469-3479.	3.3	28
94	The tectonics of the western Ordos Plateau, Ningxia, China: Slip rates on the Luoshan and East Helanshan Faults. Tectonics, 2016, 35, 2754-2777.	2.8	27
95	Interseismic strain accumulation across the Manyi fault (Tibet) prior to the 1997 M _{<i>w</i>} 7.6 earthquake. Geophysical Research Letters, 2011, 38, n/a-n/a.	4.0	26
96	Geoid lineations of 1000 km wavelength over the central Pacific. Geophysical Research Letters, 1995, 22, 97-100.	4.0	25
97	Scaling of viscous shear zones with depth-dependent viscosity and power-law stress–strain-rate dependence. Geophysical Journal International, 2015, 202, 242-260.	2.4	25
98	The effect of a shallow low-viscosity zone on the mantle flow, the geoid anomalies and the geoid and depth-age relationships at fracture zones. Geophysical Journal International, 1988, 93, 25-43.	2.4	24
99	Cooling of the oceanic lithosphere—evidence from geoid anomalies across the Udintsev and Eltanin fracture zones. Earth and Planetary Science Letters, 1988, 88, 289-307.	4.4	24
100	Characterizing Complex Surface Ruptures in the 2013 <i>M</i> _{<i>w</i>} 7.7 Balochistan Earthquake Using Threeâ€Dimensional Displacements. Journal of Geophysical Research: Solid Earth, 2018, 123, 10,191.	3.4	22
101	Radar interferometry time series analysis of Mashhad subsidence. Journal of the Indian Society of Remote Sensing, 2009, 37, 147-156.	2.4	20
102	Largeâ€Scale Interseismic Strain Mapping of the NE Tibetan Plateau From Sentinelâ€1 Interferometry. Journal of Geophysical Research: Solid Earth, 2022, 127, .	3.4	17
103	Mapping 3D fault geometry in earthquakes using highâ€resolution topography: Examples from the 2010 El Mayorâ€Cucapah (Mexico) and 2013 Balochistan (Pakistan) earthquakes. Geophysical Research Letters, 2016, 43, 3134-3142.	4.0	16
104	Geoid anomalies over two South Atlantic fracture zones. Earth and Planetary Science Letters, 1990, 100, 18-41.	4.4	15
105	The Relationship Between Seismic and Aseismic Slip on the Philippine Fault on Leyte Island: Bayesian Modeling of Fault Slip and Geothermal Subsidence. Journal of Geophysical Research: Solid Earth, 2020, 125, e2020JB020052.	3.4	15
106	The inverse problem of constructing a gravimetric geoid. Journal of Geophysical Research, 1982, 87, 1835-1848.	3.3	11
107	Comparison of seismic and geodetic strain rates at the margins of the Ordos Plateau, northern China. Geophysical Journal International, 2018, 212, 988-1009.	2.4	10
108	Co-seismic vertical displacements from a single post-seismic lidar DEM: example from the 2010 El Mayor-Cucapah earthquake. Geophysical Journal International, 2015, 202, 328-346.	2.4	8

#	Article	IF	CITATIONS
109	Postâ€Earthquake Fold Growth Imaged in the Qaidam Basin, China, With Interferometric Synthetic Aperture Radar. Journal of Geophysical Research: Solid Earth, 2021, 126, e2020JB021241.	3.4	8
110	A comparison of discrete and continuous intrusion models for the thermal structure of the plates. Geophysical Journal of the Royal Astronomical Society, 1982, 70, 741-753.	0.2	7
111	A detailed gravity field over the Reykjanes Ridge from Seasat, Geosat, ERS-1 and TOPEX/POSEIDON altimetry and shipborne gravity. Geophysical Research Letters, 1994, 21, 2841-2844.	4.0	5
112	Reply [to "Comments on â€~Comparison of long-wavelength residual elevation and free air gravity anomalies in the North Atlantic and possible implications for the thickness of the lithospheric plate' by John G. Sclater, Lawrence A. Lawver, and Barry Parsonsâ€: Journal of Geophysical Research, 1976, 81, 4960-4964.	3.3	4
113	Gravity fields over mid-ocean ridges from GEOSAT GM data: Variations as a function of spreading rate. Geophysical Research Letters, 1994, 21, 2837-2840.	4.0	4
114	Reply [to "Comment on â€~Geodetic investigation of the 13 May Kozani-Grevena (Greece) Earthquake' by Clarke et al.â€]. Geophysical Research Letters, 1998, 25, 131-133.	4.0	4